Photoelectron spectroscopy and density functional calculations of $Cu_nBO_2(OH)^-$ ($n = 1,2$) clusters

Yuan Feng [a,b], Gao-Lei Hou [a], Hong-Guang Xu [a], Zeng-Guang Zhang [a], Wei-Jun Zheng [a,*]

[a] Beijing National Laboratory for Molecular Sciences, State Key Laboratory of Molecular Reaction Dynamics, Institute of Chemistry, Chinese Academy of Sciences, Beijing 100190, China
[b] School of Electronics and Information Engineering, Hefei Normal University, Hefei 230601, China

ARTICLE INFO

ABSTRACT

$Cu_nBO_2(OH)^-$ ($n = 1, 2$) clusters were studied by anion photoelectron spectroscopy and density functional calculations. From the experimental photoelectron spectra, the adiabatic detachment energy (ADE) and vertical detachment energy (VDE) of $CuBO_2(OH)^-$ are determined to be 4.00 ± 0.08 and 4.26 ± 0.08 eV, and those of $Cu_2BO_2(OH)^-$ to be 2.30 ± 0.08 and 2.58 ± 0.08 eV. The structures of $Cu_nBO_2(OH)^-$ and their corresponding neutrals are assigned by comparison between theoretical calculations and experimental measurements. Both experiment and theory show that $CuBO_2(OH)$ can be viewed as a superhalogen, thus, confirmed that OH can behave like a halogen atom to participate in superhalogen formation.

1. Introduction

The term of superhalogen was first proposed by Gutsev and Boldyrev to classify a series of extraordinary species with electron affinities (EAs) higher than those of halogen atoms (F, Cl, Br, and I) [1,2]. Since superhalogens may serve as building blocks for new materials [3,4], they have received great attention in recent years. Numerous of superhalogens have been studied during the past two decades [5–20]. Among them, BO_2 has been confirmed to behave as a superhalogen because of its high electron affinity and special electronic property [21,22]. Moreover, it has been shown by experiments and/or theoretical calculations that BO_2 can serve as a building block to participate in the formation of more electronegative superhalogens (or hyperhalogens), such as $Au_{2,4}(BO_2)$ [23], $Au(BO_2)_2$ [24], $Cu(BO_2)_2$ [25], and $Al(BO_2)_4$ [26]. Very recently, extensive efforts have been devoted to search for alternative ligands or building blocks which might be suitable for the formation of novel superhalogens [27–29]. OH radical has nine electrons and is isoelectronic with F atom. Although the EA of OH (1.827 eV [30]) is much lower than that of F atom (3.40 eV [31]), it has been proposed that OH is also capable of serving as a ligand to form superhalogen anions in a series of metal hydroxides, $M(OH)_{k+1}^-$ (M = Li, Na, K; Be, Mg, Ca; B, Al, Ga. k is the maximal formal valence of M) [28,29]. Theoretical calculations also suggested that superhalogens composed of mixed ligands may have different properties compared to those composed of the same type of ligands [32]. Since we investigated $Cu(BO_2)_2$ previously [25], it would be interesting to see whether it is possible to form superhalogens with both BO_2 and OH as ligands. On the other hand, OH is one of the most impor-

tant sources of bases in solution chemistry [33–35] and environmental chemistry [36–38]. Understanding the interaction between OH and $CuBO_2$ might be useful for making transparent conductive devices because $CuBO_2$ is an important p-type transparent oxide in the Cu-delafossite family [39] and the preparation and applications of $CuBO_2$ may be affected by OH radical in the environment. In this work, we conducted a combined photoelectron spectroscopy and density functional theory study on the structures and electronic properties of $CuBO_2(OH)^-$ and $Cu_2BO_2(OH)^-$ clusters to understand the interactions between OH and Cu_nBO_2 clusters and possible formation of superhalogen by OH.

2. Experimental and computational methods

2.1. Experimental methods

The experiments were conducted using a home-built apparatus consisting of a time-of-flight (TOF) mass spectrometer and a magnetic-bottle photoelectron spectrometer, which has been described in detail elsewhere [40]. Briefly, a rotating and translating disk target of Cu/B alloy (13 mm diameter, Cu/B mole ratio 50:1) was ablated with the second harmonic (532 nm) light pulses from an Nd:YAG laser (Continuum Surelite II-10). The laser-induced plasma was mixed with helium carrier gas which was allowed to expand into the source through a pulsed valve (General Valve Series 9) with ~4 atm backing pressure. The trace amounts of water and oxygen in the carrier gas or on the target surface can serve as sources of OH and oxygen for the formation of $Cu_nBO_2(OH)^-$ clusters. The cluster anions were mass analyzed by the TOF mass spectrometer. The $Cu_nBO_2(OH)^-$ ($n = 1,2$) clusters were mass-selected and decelerated before being photodetached by a second laser beam. Two types of photon energies, 266 nm (4.661 eV) from an

* Corresponding author. Fax: +86 10 62563167.
E-mail address: zhengwj@iccas.ac.cn (W.-J. Zheng).

Nd: YAG laser and 193 nm (ArF, 6.424 eV) from an excimer laser, were used for photodetachment in this work. The photodetached electrons were collected and energy-analyzed by the magnetic-bottle photoelectron spectrometer. The photoelectron spectra were calibrated using the known spectrum of Cu^-. The instrumental resolution was approximately 40 meV for electrons with 1 eV kinetic energy.

2.2. Computational methods

The theoretical calculations were performed employing the B3LYP functional [41,42] implemented in the GAUSSIAN 09 program package [43]. The 6-311+G(d, p) basis set was used for H, B, O, and Cu atoms. The theoretical method was tested by calculating the electron affinities of Cu_2, CuO, BO, and OH. The calculations show that the electron affinities of Cu_2, CuO, BO, and OH are 0.85, 1.52, 2.60, and 1.77 eV respectively, in good agreement with the experimental values in the literature (0.836 eV for Cu_2 [44], 1.777 eV for CuO [45], 2.510 eV for BO [21], and 1.827 eV for OH [30]). The geometric optimizations of $Cu_nBO_2(OH)^-$ (n = 1,2) clusters as well as their corresponding neutrals were conducted without any symmetry constraint using all possible initial structures. The harmonic vibrational frequencies were calculated to make sure that the structures correspond to real local minima. The calculated energies were corrected by the zero-point vibrational energies. The theoretical vertical detachment energies (VDEs) were calculated as the energy differences between the neutrals and anions both at the geometries of the anionic species. The theoretical adiabatic detachment energies (ADEs) were calculated as the energy differences between the neutrals and anions with the neutral structures relaxed to the nearest local minima using the geometries of the corresponding anions as initial structures.

3. Experimental results

Figure 1 shows a typical mass spectrum obtained in our experiments. As shown in the spectrum, the mass peaks of the produced species are relatively complicated due to the isotopic distributions of copper and boron, but the mass assignments can be made unambiguously by analyzing the isotope abundances of the cluster anions.

The photoelectron spectra of $Cu_nBO_2(OH)^-$ (n = 1,2) taken at 266 nm (4.661 eV) and 193 nm (6.424 eV) are presented in Figure 2. The adiabatic detachment energies (ADEs) and vertical detachment energies (VDEs) estimated from the photoelectron spectra are
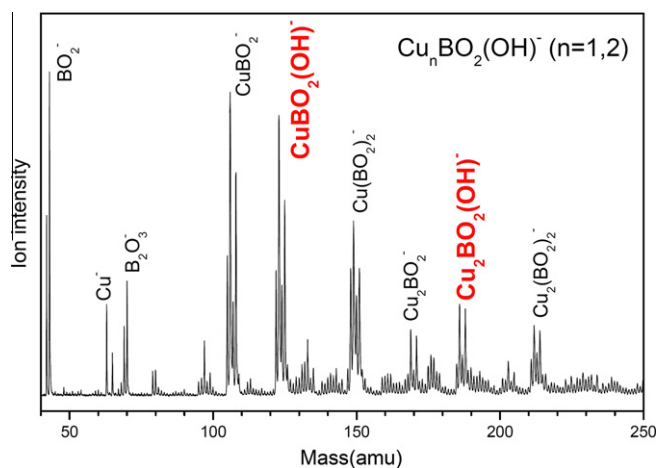
summarized in Table 1. To account for the broadening of the photoelectron spectrum due to the instrumental resolution, the ADEs were determined by adding the value of instrumental resolution to the onsets of the first peaks in the spectra. The onsets of the first peaks were found by drawing a straight line along the leading edge of the peaks to cross the baseline of the spectra.

In the 266 nm spectrum of $CuBO_2(OH)^-$ (Figure 2a), only an onset of the photoelectron feature is observed near the 266 nm photon energy limit due to the expected high electron binding energy of $CuBO_2(OH)^-$. In the 193 nm spectrum, a full band feature centered at ∼4.26 eV along with two more discernible features at about 4.8 and 5.6 eV are observed.

For $Cu_2BO_2(OH)^-$ (Figure 2b), a peak centered at ∼2.58 eV is observed in the 266 nm spectrum. In its 193 nm spectrum, some structureless features can be observed at the higher electron binding energy side in addition to the 2.58 eV feature detected in the 266 nm spectrum. The high binding energy features are relatively hard to be distinguished due to the poor signal to noise ratio in the 193 nm spectrum.

4. Theoretical results and discussion

To investigate the geometric structures and electronic properties of $Cu_n(BO_2)(OH)^-$ (n = 1,2) clusters, we performed density functional calculations on these cluster anions and their corresponding neutrals. The optimized geometries of the low-lying isomers of $Cu_nBO_2(OH)^-$ (n = 1,2) and their corresponding neutrals are presented in Figure 3 with the most stable isomers on the left. The relative energies between these isomers as well as the ADEs and VDEs from theoretical calculations are summarized in Table 1 along with the experimental ADEs and VDEs.

4.1. $CuBO_2(OH)^-$ and $CuBO_2(OH)$

As seen in Figure 3, the ground state geometry of $CuBO_2(OH)^-$ cluster, isomer 1A, is a chain structure with a central Cu atom interacting with a BO_2 unit on one side and an OH unit on the other side. The calculated ADE and VDE of isomer 1A are 3.91 and 4.04 eV, respectively, in good agreement with the experimental values. Isomer 1B can be obtained by attaching the OH moiety to the B atom of a Cu–O–B–O four-membered ring. Isomer 1C is formed by attaching the OH moiety to the B atom of a distorted Cu–O–B–O chain. Isomers 1B and 1C are much higher in energy (ΔE > 1.7 eV) than isomer 1A. The theoretical ADEs and VDEs of both isomers 1B and 1C are much lower than the experimental measurements. Therefore, isomer 1A is suggested to be the most probable structure of $CuBO_2(OH)^-$ present in our experiments.

The optimized ground state structure of the neutral $CuBO_2(OH)$ (isomer 1A′) is nearly identical to its anionic counterpart with only small changes in the bond lengths. These changes probably can be attributed to the increasing of the interaction between Cu and O atoms of both BO_2 and OH moiety in the neutral. The structures of isomers 1B′ and 1C′ are also similar to their corresponding anions.

4.2. $Cu_2BO_2(OH)^-$ and $Cu_2BO_2(OH)$

The first two isomers of $Cu_2BO_2(OH)^-$ anions, isomers 2A and 2B, can be considered as derived from isomer 1A. Isomer 2A is formed by attaching the second Cu atom to the O atom of OH unit of isomer 1A, while isomer 2B is formed by attaching the second Cu atom to the O end of the BO_2 unit of isomer 1A. Isomer 2B is higher in energy than isomer 2A by 0.28 eV, indicating that the second Cu atom prefers to bond to the OH unit. Isomer 2C is a linear structure with a central Cu_2 unit interacting with a BO_2 unit on one side and
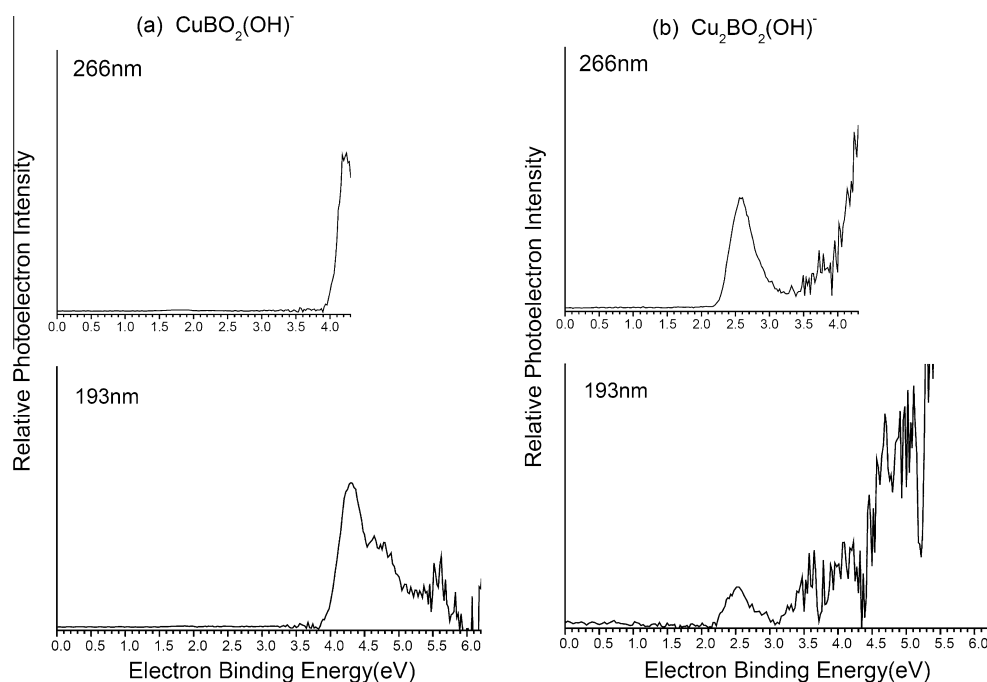

Figure 1. Mass spectrum of $Cu_nBO_2(OH)^-$ cluster anions.

Figure 2. Photoelectron spectra of $Cu_nBO_2(OH)^-$ (n = 1,2) clusters recorded with 266 nm and 193 nm photons.

Table 1
Relative energies of the low energy isomers of $Cu_nBO_2(OH)^-$ (n = 1,2) calculated with the B3LYP method and 6–311 + G(d, p) basis set as well as the comparison of their theoretical ADEs and VDEs to the experimental values. The isomers labeled in bold are the most probable structures in the experiments.

Clusters	Isomers	ΔE (eV)	State	Sym.	ADE (eV)		VDE (eV)	
					Theo.	Exp.	Theo.	Exp.
$CuBO_2(OH)^-$	1A	0.00	^1A	C_1	3.91	4.00 ± 0.08	4.04	4.26 ± 0.08
	1B	1.72	$^1A'$	C_s	2.22		2.56	
	1C	2.26	$^1A'$	C_s	2.43		2.72	
$Cu_2BO_2(OH)^-$	2A	0.00	^2A	C_1	2.52	2.30 ± 0.08	2.73	2.58 ± 0.08
	2B	0.28	^2A	C_1	2.74		2.88	
	2C	0.45	^2A	C_1	2.07		4.09	
	2D	0.50	^2A	C_1	2.60		2.88	

an OH unit on the other side. It is higher in energy than isomer 2A by 0.45 eV. The VDE of isomer 2C is calculated to be 4.09 eV. This high VDE is resultant from the high energy of its corresponding neutral instead of its superhalogen behavior. Isomer 2D is formed by attaching the second Cu atom to the O atom between B and Cu in the O–B–O–Cu–O–H chain. The theoretical ADE and VDE of isomer 2A are calculated to be 2.52 and 2.73 eV respectively, in accord well with the experimental values of 2.30 and 2.58 eV. The calculated VDEs of the higher energy isomers (2B-2D) are much higher than the experimental values. Therefore, isomer 2A is the most probable structure detected in the experiments.

The ground state geometry of the neutral $Cu_2BO_2(OH)$ cluster (isomer 2A′), unlike its anionic counterpart, is not chain-like, but an six-membered ring structure composed of two Cu atoms, a O–B–O unit, and the oxygen atom of OH unit. Isomer 2B′ is formed by attaching the second Cu atom to the O atom of OH unit in the O–B–O–Cu–O–H chain. Isomer 2B′ is higher in energy than isomer 2A′ by 0.82 eV. Isomer 2C' has both Cu atoms bridging the OH and BO_2 units, therefore, its central part is a rhombus formed by two Cu atoms and two O atoms. Isomer 2D′ can be considered as a B atom interacting with an OH unit and two OCu units via the O atoms. The energies of isomer 2C′ and 2D′ are 0.99 and 1.15 eV higher than that of isomer 2A′.

5. Discussion

The VDE of $CuBO_2$ has been measured to be ∼2.12 eV in the previous work [25]. Addition of an OH unit to $CuBO_2$ increases the VDE significantly to 4.26 eV. The increased value is larger than the electron affinity of OH (1.827 eV [30]). Since the structures of $CuBO_2(OH)^-$ and $CuBO_2(OH)$ are nearly identical, the EA of $CuBO_2(OH)$ can be considered as equal to the ADE of $CuBO_2(OH)^-$ (4.00 ± 0.08 eV), which is larger than the EA of chlorine atom (3.62 eV). In addition to its high EA exceeding that of chlorine, $CuBO_2(OH)$ is one electron short to electronic shell-closing. These facts imply that $CuBO_2(OH)$ has the characters of superhalogen.

It is also interesting to compare $Cu_nBO_2(OH)^-$ (n = 1, 2) with $Cu_n(BO_2)_2^-$ (n = 1, 2) clusters. Our previous study show that the VDE of $Cu(BO_2)_2^-$ is about 5.28 eV and that of $Cu_2(BO_2)_2^-$ is about 2.92 eV [25]. The VDE of $CuBO_2(OH)^-$ is lower than that of $Cu(BO_2)_2^-$ by ∼1.02 eV, whereas the VDE of $Cu_2BO_2(OH)^-$ is lower than that of $Cu_2(BO_2)_2^-$ by ∼0.34 eV. Our theoretical calculations show that the structures of $Cu_nBO_2(OH)^-$ (n = 1, 2) (Figure 3) can be regarded as simply replacing one of the BO_2 uint in $Cu_n(BO_2)_2^-$ (n = 1, 2) by an OH unit. The introducing of OH into the clusters causes only minor perturbation on the geometric structure of $CuBO_2$. Since the electron affinity of OH is much lower than that
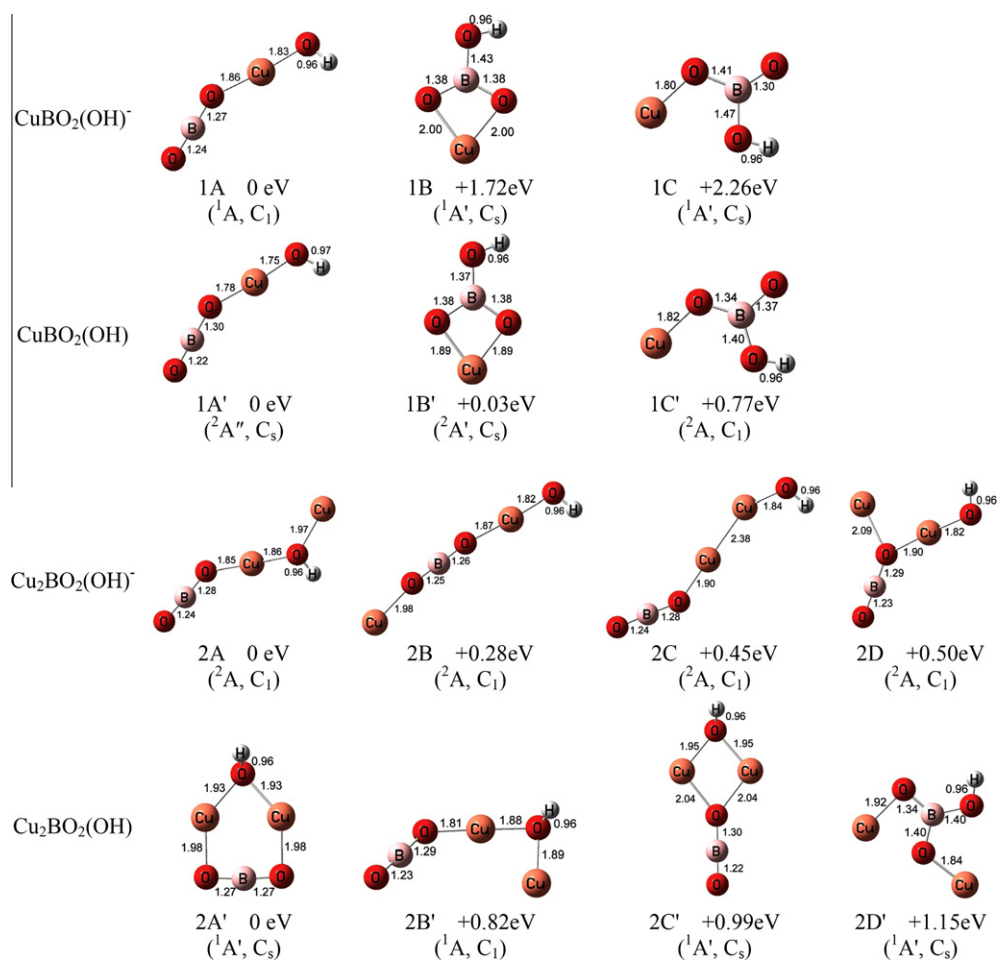
Figure 3. Optimized low-lying isomers of $Cu_nBO_2(OH)^-$ ($n = 1,2$) cluster anions and their corresponding neutrals. The bond lengths are labeled in the geometric structures.
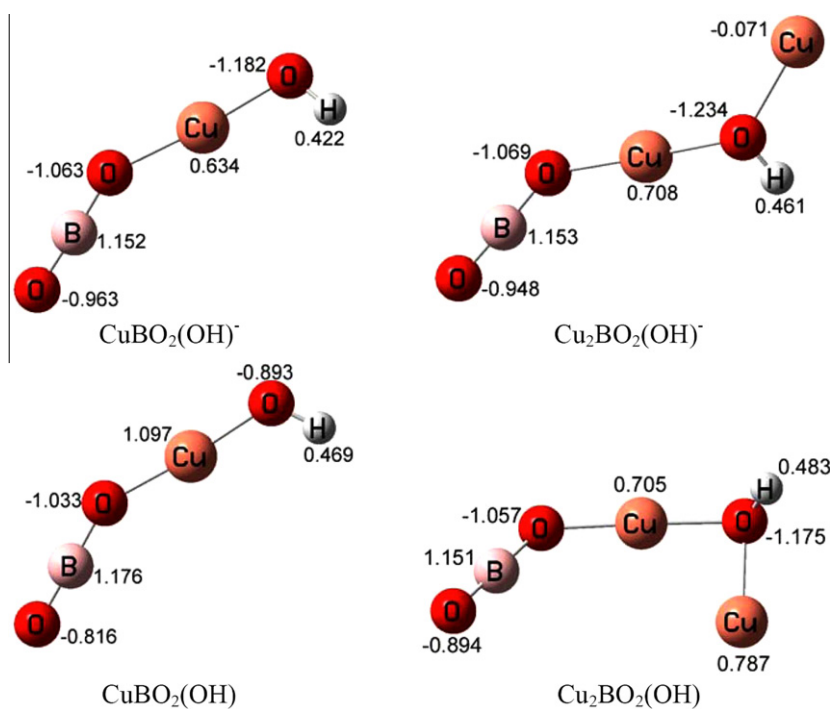

Figure 4. Natural bond orbital (NBO) charge distributions of the ground state of $Cu_nBO_2(OH)^-$ ($n = 1,2$) clusters and their corresponding neutrals.

of BO_2, it is reasonable that the VDEs shift toward lower values when a BO_2 is replaced by an OH unit. As $Cu(BO_2)_2$ has been proposed to be a superhalogen or hyperhalogen [25], the reduction of VDE due to introducing of OH unit is also consistent with the theoretical calculations of Smuczyńska and Skurski [32], who suggested that introducing of various halogen ligands into the superhalogens would change the nature of the HOMO, therefore, reduce their electronic stabilities.

The natural bond orbital (NBO) charge distributions of $Cu_nBO_2(OH)^-$ ($n = 1,2$) and their corresponding neutrals are shown in Figure 4. By comparing NBO charge distribution of $CuBO_2(OH)^-$ to that of neutral $CuBO_2(OH)$ cluster, we can see that the excess electron delocalizes over the entire cluster with about 46% on the Cu atom, 20% on the BO_2 unit and 34% on the OH moiety. This is also consistent with the superhalogen properties of $CuBO_2(OH)$. From the charge distributions of $Cu_2BO_2(OH)^-$ and $Cu_2BO_2(OH)$ clusters, we can see that the excess electron of $Cu_2BO_2(OH)^-$ mainly localizes on the terminal Cu atom bonding to the OH unit, which is also compatible with the superhalogen properties of $CuBO_2(OH)$. If we consider $[CuBO_2(OH)]$ as a halogen atom (X) and $Cu_2BO_2(OH)$ as a Cu^+X^- molecule, the localization of the excess electron on the terminal Cu atom is very similar to the formation of anions in the case of copper(I) halides and alkali halides, in which the excess electron mainly localizes on the positive pole of the dipole of halide molecule since it is repulsed by the negative pole.

In summary, our experimental measurements and density functional calculations on $Cu_nBO_2(OH)^-$ ($n = 1,2$) clusters show that OH can behave like a halogen atom to participate in the formation of superhalogens although its electron affinity is much lower than those of halogens. This is also in agreement with Anusiewicz and coworkers' theoretical calculations that nine-electron ligands such as OH are good candidates for playing ligand roles in the formation of superhalogens [28,29].

6. Conclusions

We conducted a combined photoelectron spectroscopy and density functional study on $Cu_nBO_2(OH)^-$ ($n = 1,2$) clusters and their corresponding neutrals. The adiabatic and vertical detachment energies of $Cu_nBO_2(OH)^-$ were determined from their photoelectron spectra. Based on the optimized geometries, NBO charge distributions, and comparison with $Cu_nBO_2(BO_2)^-$, we found that the OH group bonds to Cu_nBO_2 in a similar manner as BO_2 and causes very little change to the geometries of Cu_nBO_2. The $Cu_nBO_2(OH)^-$ ($n = 1,2$) clusters have much lower electron binding energies than $Cu_nBO_2(BO_2)^-$ due to the smaller size and lower EA of OH relative to BO_2. Still, $CuBO_2(OH)$ can be regarded as a superhalogen because its EA is higher than that of chlorine atom. Our study confirmed the theoretical predictions that OH can behave like a halogen atom in the formation of superhalogens although its EA is much lower than those of halogens.

Acknowledgements

References

[1] G.L. Gutsev, A.I. Boldyrev, Chem. Phys. 56 (1981) 277.
[2] G.L. Gutsev, A.I. Boldyrev, Chem. Phys. Lett. 108 (1984) 250.
[3] S.A. Claridge, A.W. Castleman, S.N. Khanna, C.B. Murray, A. Sen, P.S. Weiss, ACS Nano 3 (2009) 244.
[4] A.W. Castleman, S.N. Khanna, J. Phys. Chem. C 113 (2009) 2664.
[5] X.-B. Wang, C.-F. Ding, L.-S. Wang, A.I. Boldyrev, J. Simons, J. Chem. Phys. 110 (1999) 4763.
[6] G.L. Gutsev, B.K. Rao, P. Jena, X.-B. Wang, L.-S. Wang, Chem. Phys. Lett. 312 (1999) 598.
[7] X. Yang, X.-B. Wang, L.-S. Wang, S. Niu, T. Ichiye, J. Chem. Phys. 119 (2003) 8311.
[8] A.N. Alexandrova, A.I. Boldyrev, Y.-J. Fu, X. Yang, X.-B. Wang, L.-S. Wang, J. Chem. Phys. 121 (2004) 5709.
[9] D.E. Bergeron, A.W. Castleman, T. Morisato, S.N. Khanna, Science 304 (2004) 84.
[10] B.M. Elliott, E. Koyle, A.I. Boldyrev, X.-B. Wang, L.-S. Wang, J. Phys. Chem. A 109 (2005) 11560.
[11] F.-F. Wang, Z.-R. Li, D. Wu, X.-Y. Sun, W. Chen, Y. Li, C.-C. Sun, ChemPhysChem 7 (2006) 1136.
[12] J. Yang, X.-B. Wang, X.-P. Xing, L.-S. Wang, J. Chem. Phys. 128 (2008) 201102.
[13] S. Smuczyńska, P. Skurski, Inorg. Chem. 48 (2009) 10231.
[14] Q. Wang, Q. Sun, P. Jena, J. Chem. Phys. 131 (2009) 124301.
[15] J. Joseph, S. Behera, P. Jena, Chem. Phys. Lett. 498 (2010) 56.
[16] K. Pradhan, G.L. Gutsev, P. Jena, J. Chem. Phys. 133 (2010) 144301.
[17] Y.J. Ko, H. Wang, K. Pradhan, P. Koirala, A.K. Kandalam, K.H. Bowen, P. Jena, J. Chem. Phys. 135 (2011) 244312.
[18] B. Pathak, D. Samanta, R. Ahuja, P. Jena, ChemPhysChem 12 (2011) 2423.
[19] M.M. Wu et al., Angew. Chem. Int. Ed. 50 (2011) 2568.
[20] J. Joseph, K. Pradhan, P. Jena, H. Wang, X. Zhang, Y. Jae Ko, K.H. Bowen, J. Chem. Phys. 136 (2012) 194305.
[21] H.-J. Zhai, L.-M. Wang, S.-D. Li, L.-S. Wang, J. Phys. Chem. A 111 (2007) 1030.
[22] Y. Feng, H.-G. Xu, Z.-G. Zhang, Z. Gao, W.-J. Zheng, J. Chem. Phys. 132 (2010) 074308.
[23] M. Götz, M. Willis, A.K. Kandalam, G.F. Ganteför, P. Jena, ChemPhysChem 11 (2010) 853.
[24] M. Willis, M. Götz, A.K. Kandalam, G.F. Ganteför, P. Jena, Angew. Chem. Int. Ed. 49 (2010) 8966.
[25] Y. Feng, H.-G. Xu, W.-J. Zheng, H.-M. Zhao, A.K. Kandalam, P. Jena, J. Chem. Phys. 134 (2010) 094309.
[26] G.L. Gutsev, C.A. Weatherford, L.E. Johnson, P. Jena, J. Comput. Chem. 33 (2012) 416.
[27] I. Anusiewicz, J. Phys. Chem. A 113 (2009) 11429.
[28] C. Sikorska, S. Freza, P. Skurski, I. Anusiewicz, J. Phys. Chem. A 115 (2011) 2077.
[29] I. Świerszcz, I. Anusiewicz, Chem. Phys. 383 (2011) 93.
[30] J.D. Rudmin, L.P. Ratliff, J.N. Yukich, D.J. Larson, J. Phys. B 29 (1996) L881.
[31] H. Hotop, W.C. Lineberger, J. Phys. Chem. Ref. Data 14 (1985) 731.
[32] S. Smuczyńska, P. Skurski, Chem. Phys. Lett. 452 (2008) 44.
[33] C. Anastasio, J.T. Newberg, J. Geophys. Res. 112 (2007) D10306.
[34] R. von Glasow, Atmos. Chem. Phys. 6 (2006) 3571.
[35] R. Hell, U.W. Stephan, Planta 216 (2003) 541.
[36] A.A.P. Pszenny et al., Geophys. Res. Lett. 20 (1993) 699.
[37] C.J. Christiansen, S.S. Dalal, J.S. Francisco, A.M. Mebel, J.S. Gaffney, J. Phys. Chem. A 114 (2010) 2806.
[38] D. Cappus et al., Chem. Phys. 177 (1993) 533.
[39] M. Snure, A. Tiwari, Appl. Phys. Lett. 91 (2007) 092123.
[40] H.-G. Xu, Z.-G. Zhang, Y. Feng, J.-Y. Yuan, Y.-C. Zhao, W.-J. Zheng, Chem. Phys. Lett. 487 (2010) 204.
[41] A.D. Becke, J. Chem. Phys. 98 (1993) 5648.
[42] C. Lee, W. Yang, R.G. Parr, Phys. Rev. B 37 (1988) 785.
[43] M.J. Frisch, G.W. Trucks, H.B. Schlegel, Gaussian 09, in, Gaussian Inc. Wallingford CT, 2009.
[44] C.L. Pettiette, S.H. Yang, M.J. Craycraft, J. Conceicao, R.T. Laaksonen, O. Cheshnovsky, R.E. Smalley, J. Chem. Phys. 88 (1988) 5377.
[45] M.L. Polak, M.K. Gilles, J. Ho, W.C. Lineberger, J. Phys. Chem. 95 (1991) 3460.